

Extremely wide-angle lens with transmissive and catadioptric integration

XIAOHENG WANG,^{1,2} XING ZHONG,^{1,2,3,*} RUIFEI ZHU,^{2,3} FANG GAO,³ AND ZHUQIANG LI³

¹Changchun Institute of Optics, Fine Mechanics and Physics, Chinese Academy of Sciences, Changchun 130033, China

²University of Chinese Academy of Sciences, Beijing 100049, China

³Chang Guang Satellite Technology CO, LTD, Key Laboratory of Satellite Remote Sensing Application, Changchun 130012, China

*Corresponding author: wangxiaoheng0013@163.com

Received 26 March 2019; revised 6 May 2019; accepted 6 May 2019; posted 7 May 2019 (Doc. ID 363413); published 29 May 2019

Wide-angle lenses can be generally classified into two structures: a transmitted fish-eye structure and a catadioptric structure with a panoramic annular lens (PAL). Compared with the former, the latter exhibits better imaging capability for a super-large field of view. However, the PAL causes this type of optical system to lose its imaging ability in a small field of view in front of the lens. In this study, a novel extremely wide-angle lens is designed by combining the fish-eye and catadioptric structures. The designed lens integrates the transmissive and catadioptric structures and can simultaneously observe two fields of view. The two fields of view of the lens complement each other and completely eliminate the central observation blind area of ordinary catadioptric wide-angle lens. The forward field of view of the lens is $360^\circ \times (0^\circ - 56^\circ)$, and the annular field of view is $360^\circ \times (55^\circ - 115^\circ)$. The total field of view of the optical system reaches 230° when only spherical lenses are used for all the optical elements. The optical model shows that the imaging quality of the extremely wide-angle lens is good, which proves the advantages of the new optical system in a large field of view. © 2019 Optical Society of America

<https://doi.org/10.1364/AO.58.004381>

1. INTRODUCTION

With the advent of the information society, people intend to gain a comprehensive grasp of information about space. Panoramic imaging technology can record a wide spatial range, which considerably facilitates the acquisition of 3D spatial information [1–3]. Panoramic imaging technology is generally divided into two types: scanning and direct viewing. Scanning panoramic technology refers to the scanning of the surrounding environment through the rotation of an imaging lens driven by a mechanical motion device to obtain images in various directions. The images are then combined through image stitching and fusion technology to obtain panoramic information of 3D space. Direct-viewing panoramic technology refers to the recording of a large space by an extremely wide-angle lens in real time. Compared with scanning panoramic technology, direct-viewing panoramic imaging is more time-efficient and does not require mechanical motion devices and postprocessing. An extremely wide-angle lens is the core device in direct-viewing panoramic technology. Commonly used wide-angle lenses have either a transmissive fish-eye structure or a catadioptric structure with a panoramic annular lens (PAL); the field angles of both structures can reach approximately 180° [4–6].

The structure of a fish-eye lens is shown in Fig. 1. The first or the first two lenses are meniscus negative lenses for

compressing the beam of a large field of view (FoV) in front of the lens. Fish-eye lenses have been studied for a long time and are frequently used to detect large paces [7,8]. In contrast with the long history of the fish-eye lens, the catadioptric wide-angle lens has been developing rapidly in the past 20 years [9,10]. The structure of a catadioptric wide-angle lens is shown in Fig. 2. This optical system uses a PAL consisting of 3 or 4 different surfaces to receive the beam from a large FoV, and the beam leaves after two reflections inside the PAL. The process of two foldbacks inside the PAL effectively compresses the aperture of the incident beam. Compared to the fully transmissive fish-eye structure, the catadioptric wide-angle lens has a better imaging capability in the large FoV, and its image quality is higher than that of the fish-eye lens. In addition, the powerful compression feature of PAL makes the catadioptric lens more easily reach the telecentric state. However, the special structure of a PAL also blocks the beam in front of the lens from entering the optical system, which makes the front FoV of the lens a blind zone for observation.

In the past, catadioptric lenses have been developed to widen the FoV and compress the blind areas. Bai *et al.* from Zhejiang University used a dichroic filter to eliminate part of the blind zone in front of a PAL [11]. Xu *et al.* from Fudan University used a free-form surface lens and a new projection relation to compress the central black spot on a detector and increase the

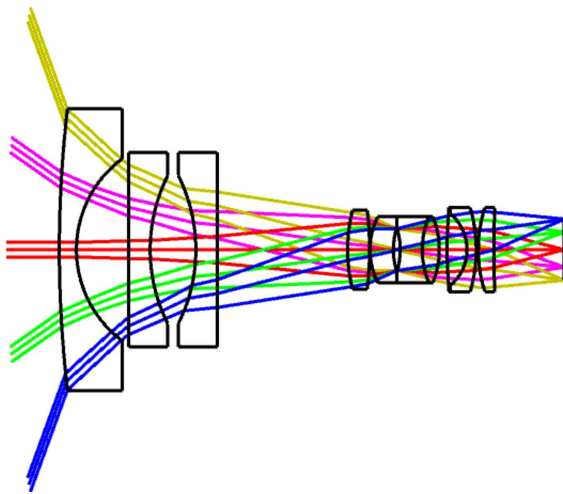


Fig. 1. Fish-eye lens.

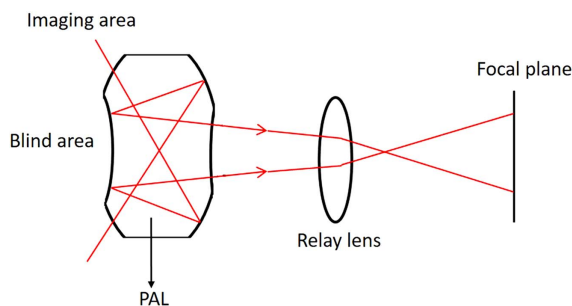


Fig. 2. Catadioptric wide-angle lens.

detector's utilization rate [12]. These studies have considerably promoted the development of panoramic imaging technology. However, both of the above methods use expensive optical components and fail to completely eliminate blind areas. Driscoll *et al.* have proposed a dual-optical-path imaging system [13]. This imaging system is a great breakthrough in function and completely eliminated the blind spot of the PAL. However, the beam of a large FoV enters the system from the rear surface of the PAL instead of the front surface, which leads to the complex mechanical structure of the optical system. In addition, the beam of a large FoV is only reflected once in the PAL, and so the ability to compress beams is limited. Therefore, a more complex relay system is required to transfer the beam, and it is difficult to achieve the telecentric state. Sheu *et al.* also proposed a dual-optical-path optical system with two half FoVs (0° – 45°) and (135° – 145°) [14]. But, the system lacks the half FoV between 45° and 135° , and does not achieve true panoramic view. M. Mizusawa of Olympus Corporation has designed an extremely wide-angle lens containing a PAL, which consists of two high-order aspheric surfaces and a conical surface [15]. The beams of a small FoV and large FoV enter the optical system from the first lens group and the PAL's conical surface, respectively. The object distance of the optical system is short, and so it is suitable for capturing images in closed and small spaces, such as for endoscopy.

At present, the majority of studies have separately considered fish-eye and catadioptric wide-angle lenses. By contrast, the current work combines the imaging principles of the fish-eye and catadioptric structures to design an extremely wide-angle lens with transmission and foldback structures. The lens has two FoVs, namely, forward and annular FoVs, from which beams entering the optical system are simultaneously imaged on the focal plane. The structure of the forward FoV is similar to that of the transmissive fish-eye lens, which has an FoV of $360^\circ \times (0^\circ$ – $56^\circ)$. Meanwhile, the annular FoV exhibits a catadioptric wide-angle structure, and its FoV is $360^\circ \times (55^\circ$ – $115^\circ)$. Using only ordinary optical components, the optical system has a total FoV of 230° and completely eliminates the blind area of ordinary catadioptric lenses. The designed optical system demonstrates the advantages in large FoV imaging, and this kind of lens has advantages in the field of large space exploration.

2. IMAGING PRINCIPLE OF A CATADIOPTIC WIDE-ANGLE LENS

An imaging optical system has two projection modes: tangent and equidistant. As shown in Fig. 3, an object with a FoV angle of 2α has varying image heights, which are produced by tangent and equidistant projections. The height difference between the images produced by the two projection modes is

$$d = f' \cdot (\tan \alpha - \alpha). \quad (1)$$

From Eq. (1), a conclusion can be drawn that $d = 0$ at $\alpha \rightarrow 0$ and d is infinite at $\alpha \rightarrow \pi/2$. The result indicates that the difference between the two projection modes increases from a small field angle to a large field angle. Most imaging systems adopt the tangent projection mode, which conforms to the visual characteristics of the human eyes. However, if the FoV of an optical system approaches 180° , then the tangent value of the half FoV is infinite, and the central projection is meaningless. Therefore, an extremely wide-angle lens must adopt the equidistant projection rule.

Most imaging systems capture the FoV in front of them. In contrast with traditional imaging instruments, a catadioptric wide-angle lens captures the image in the cylindrical region of the optical axis. As shown in Fig. 4, the field angle α on both sides of the optical axis Z is a blind zone of a catadioptric wide-angle lens, and the field angle ($\alpha \sim \beta$) is an imaging area. The optical system exhibits rotational symmetry around the optical axis Z . Thus, the FoV of the system is $360^\circ \times (\alpha \sim \beta)$. The central area of the image plane of the optical system is a

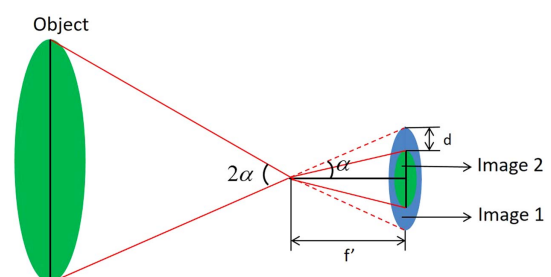


Fig. 3. Two projection modes of an imaging optical system.

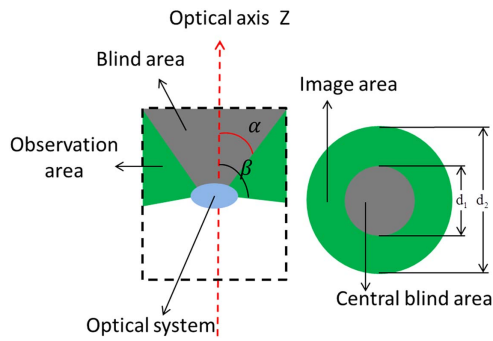


Fig. 4. Imaging mode of a catadioptric wide-angle lens.

round black spot with a diameter of d_1 , which corresponds to the observation blind area in front of a catadioptric lens. Outside the central black spot is an annular image with an outer diameter of d_2 , which corresponds to the imaging FoV of the lens. A catadioptric lens has a large FoV, which enables it to adopt an equidistant projection relationship. We set the focal length of the optical system to f' . Then, the diameter d_1 of the central black spot on the focal plane is

$$d_1 = 2 \cdot f' \cdot \alpha. \quad (2)$$

The outer diameter d_2 of the annular image is

$$d_2 = 2 \cdot f' \cdot \beta. \quad (3)$$

3. IMAGING CONCEPT OF THE EXTREMELY WIDE-ANGLE LENS WITH INTEGRATED TRANSMISSION AND FOLDBACK

The detection area of a catadioptric wide-angle lens is located on both sides of the optical axis. Hence, a catadioptric wide-angle lens has an advantage over a fish-eye lens in terms of large FoV detection. However, the black spot at the center of the image plane reduces the utilization rate of the image detector, which will result in considerable waste in the pixels of detectors, such as in a charge-coupled device. In addition, the blind area in front of the optical structure limits its application.

In the current study, we intend to design a wide-angle lens that can maintain the advantage of a catadioptric structure in a large FoV and completely eliminate the blind area in front of an optical system. Therefore, this optical system should have two FoVs, as shown in Fig. 5. The two observed FoVs of the optical system are the annular and forward FoVs. The annular FoV is a large-angle area on both sides of the optical axis, which is

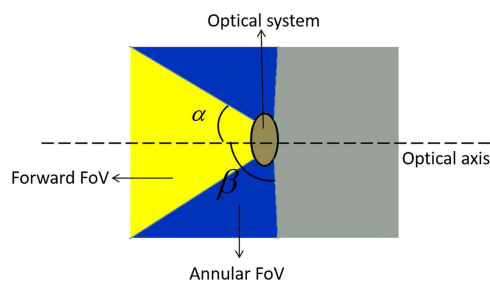


Fig. 5. Observation mode of a wide-angle lens without a blind area.

consistent with the FoV of an ordinary catadioptric wide-angle lens. The forward FoV is the zone in front of the lens, which is used to compensate for the blind area of the annular FoV. The two FoVs are complementary to each other, thereby realizing an extremely wide-angle detection without a blind area.

An ordinary catadioptric wide-angle system cannot observe a small field, because the PAL structure inside the lens is special. The structure of a PAL is shown in Fig. 6, which is composed of transmission surfaces A and B and reflection surfaces 1 and 2 [16]. The light from a large FoV enters the PAL through transmission surface A and is reflected by reflection surfaces 1 and 2 inside the PAL. The light then leaves the PAL through transmission surface B and enters the subsequent optical components. As shown in Fig. 6, reflection surface 2 blocks the light of a small FoV in front of the PAL from entering the optical system, thereby producing a blind zone. To eliminate the blind area of observation, reflection surface 2 should exhibit transmission and reflection functions. Therefore, reflection surface 2 can be transformed to a transfective or dichroic surface. However, both solutions introduce new problems. A transfective surface will cause the system to lose half of the light energy while introducing a large amount of stray light. Meanwhile, a dichroic surface has varying transmission characteristics for different bands, which distinguishes the imaging spectrum of the forward FoV from the annular FoV. This spectrum difference will result in the limited application of the optical system and will increase processing cost.

To avoid the aforementioned problem, we divide surface 2 into a reflective area and a transmissive area. As shown in Fig. 7, the central area of surface 2 is the transmissive area, and the reflective area surrounds the transmissive area. The beam of the annular large FoV is constrained to the reflective area of surface 2, whereas the beam of the forward small FoV is constrained to the transmissive area of surface 2. The transmissive and reflective properties of different regions on surface 2 are controlled by means of coating. The major function of the PAL is to transmit beams from the large FoV such that the reflective area on surface 2 will occupy a larger area than that of the transmissive area. Therefore, the central transmission area on surface 2 should not be excessively large. That is, the beam of the forward FoV should have a smaller aperture. A fish-eye lens exhibits the function of compressing the beam [17], and a meniscus lens that is similar to a fish-eye lens can be placed in front of the PAL to compress the beam. This mechanism can reduce the proportion of the transmissive area on surface 2. Figure 8(a) shows the optical structure of the wide-angle

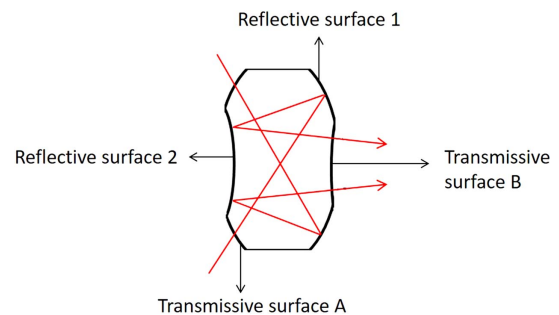


Fig. 6. PAL structure.

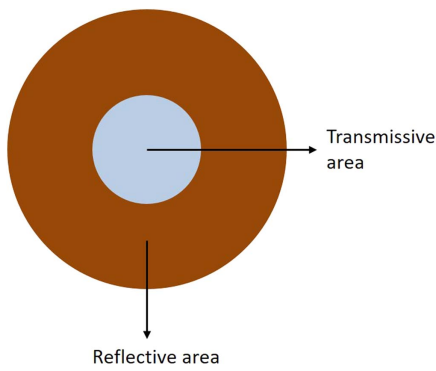


Fig. 7. Transmissive and reflective areas on surface 2 of PAL.

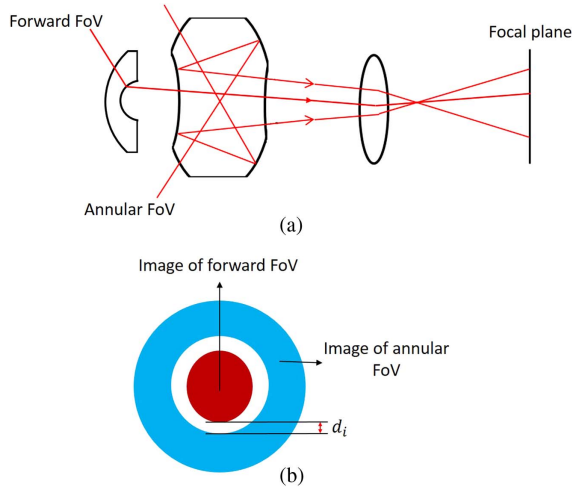


Fig. 8. Imaging concept of the wide-angle lens with integrated transmission and foldback: (a) optical structure and (b) image distribution.

lens with integrated transmission and foldback. The beam of the annular FoV enters the system from the PAL, and the beam of the forward FoV enters the PAL after being compressed by the meniscus lens, thereby realizing wide-angle detection without a blind area. The image plane of this optical system is a central bright spot, and an annular image surrounds the central bright spot, as shown in Fig. 8(b). The central bright spot and annular image are images of the forward and annular FoVs, respectively. The radii of the bright spot and annular image are determined by the focal length and field angle of the two FoVs. Distance d_i between the bright spot and the annular image is calculated using Eq. (4)

$$d_i = f_a \cdot \theta_1 - f_f \cdot \theta_2, \quad (4)$$

where f_a and f_f are the focal lengths of the annular and forward FoVs, respectively, and θ_1 and θ_2 are the minimum and maximum half-field angles of the annular and forward FoVs, respectively. The blind spot can be eliminated if θ_1 is less than or equal to θ_2 , and the d_i is created by the difference between the two foci.

4. OPTICAL DESIGN OF THE EXTREMELY WIDE-ANGLE LENS WITH TRANSMISSIVE AND CATADIOPTRIC INTEGRATION

A. PAL Design

The PAL is the core component of the entire imaging system; it is related to the success or failure of the lens design. The PAL generally consists of more than three spherical or aspherical surfaces with different curvatures; that is, the transmission and reflection surfaces on the PAL have different curvatures and aspherical coefficients [18–20]. Although a complex PAL expands the FoVs to a certain extent, it also increases processing difficulty. The structure of the PAL should be as simple as possible to reduce processing cost. We design the PAL to be consistent with a normal spherical lens. That is, the PAL consists of only two spherical surfaces with different curvatures.

Field curvature is related to the success or failure of the extremely wide-angle lens design. The Petzval sum of the entire system must be controlled to remain zero. In general, the Petzval sum of the relay optical system after the PAL is positive, and thus, the Petzval sum of the PAL is required to be less than zero. The Petzval sum of the optical system is calculated using Eq. (5)

$$P = -n_a \sum_{i=1}^m \left(\frac{1}{n'_i} - \frac{1}{n_i} \right) c_i, \quad (5)$$

where n_a is the refractive index of the last medium; c_i is the i -th surface's curvature; and n_i and n'_i are the refractive indices before and after the i -th surface, respectively. When the i -th surface is a reflective surface, $n'_i = -n_i$.

The PAL should be composed of two curvature surfaces. For the annular FoV, the curvature of the entrance and second reflection surfaces is c_1 , whereas that of the exit and first reflection surfaces is c_2 . From Eq. (5), the Petzval sum P_1 produced by the PAL is

$$\begin{aligned} P_1 &= n_a \frac{n-1}{n} c_1 + 2n_a \frac{1}{n} c_2 - 2n_a \frac{1}{n} c_1 - n_a \frac{n-1}{n} c_2 \\ &= \frac{n_a}{n} (c_1 - c_2)(n-3). \end{aligned} \quad (6)$$

As indicated in Eq. (6), when $(c_1 - c_2) > 0$, the condition in which the Petzval sum of the PAL is less than zero is satisfied. In addition, we select $c_1 > 0$ and $c_2 < 0$, considering that the front surface of the PAL should exhibit the function of compressing the beam of the annular large FoV. The shape of the PAL is shown in Fig. 9.

For the forward FoV, the Petzval sum P_2 produced by PAL is

$$P_2 = n_a \frac{n-1}{n} c_1 + n_a \frac{1-n}{n} c_2 = \frac{n_a}{n} (c_1 - c_2)(n-1). \quad (7)$$

As shown in Eq. (7), when $(c_1 - c_2) > 0$, P_2 is always greater than zero, which fails to satisfy the condition that P_2 should be less than zero. Therefore, a negative field curvature should be applied to the beam before it enters the PAL.

B. Selection of the Relay Lens and Optimization of the Catadioptric Wide-Angle Structure

After the PAL receives the beam of the annular FoV, an intermediate image with a slight negative curvature will be formed

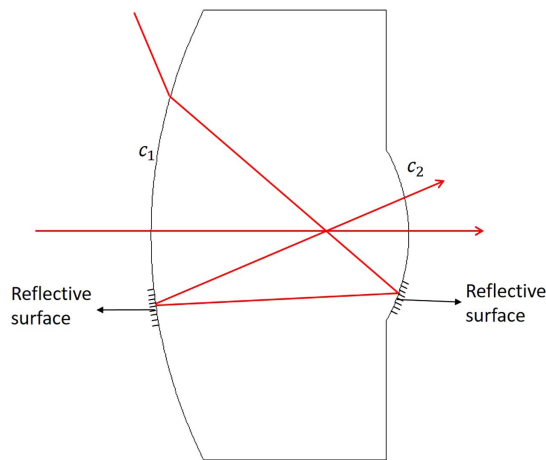


Fig. 9. Structure of the PAL.

inside PAL. A relay lens is required to focus the intermediate image onto the focal plane. In addition, the relay lens also undertakes the function of aberration correction. The intermediate image's curvature can be neglected in the process of establishing the relay lens, and the bending can be corrected by optimizing the optical system, which is spliced by the PAL and relay lens. The relay optical system group is illustrated in Fig. 10. We select the structure for splicing with the PAL and then optimize the spliced optical system. First, the relay lens is optimized. Then, the PAL is optimized under the condition that light will not overflow. Lastly, the PAL and relay lens are simultaneously optimized to ensure that the system achieves good image quality. During the optimization process, the position of light on the first surface of the PAL should be controlled such that sufficient space is allocated for the entry of the beam of the forward FoV. In addition, optimizing the exit pupil to infinity to ensure that the system is in a state of telecentricity is necessary to improve the stability of the optical system. The optimized catadioptric wide-angle structure is shown in Fig. 11. Its focal length is 5 mm, and the annular FoV of the lens is $360^\circ \times (55^\circ - 115^\circ)$. The PAL of the system has a diameter and thickness of 112 mm and 40 mm. Its material is the N-LAK8 with high hardness produced by Schott AG. The refractive index and Abbe number of the PAL are 1.71 and 53.9, respectively.

We intend to use the GSENSE400 CCD with a pixel size of $11 \mu\text{m} \times 11 \mu\text{m}$ to receive optical signals, and so the Nyquist frequency of the sensor is 45.5 l p/mm. The modulation transfer function (MTF) is shown in Fig. 12(a). In the annular FoV,

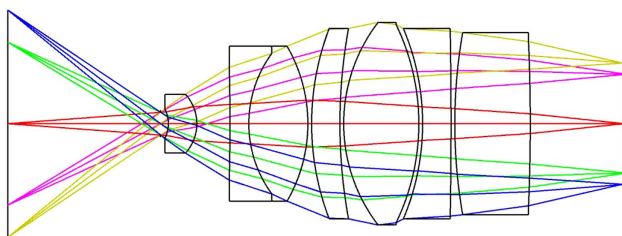


Fig. 10. Optical system of relay lens.

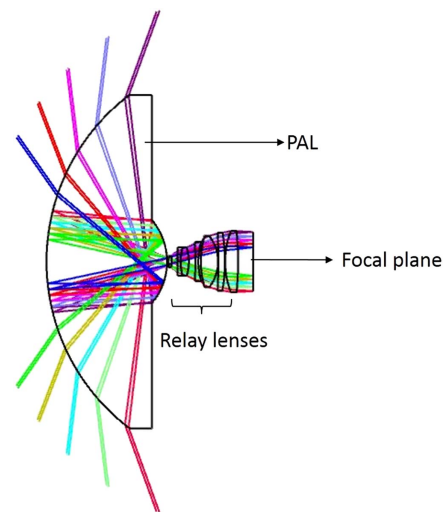


Fig. 11. Catadioptric wide-angle structure.

the MTFs of the system are higher than 0.68 at 45.5 l p/mm and 0.58 at 60 l p/mm. Therefore, the system exhibits a good contrast ratio in annular FoV. The spot diagram is shown in Fig. 12(b), and all spots have a rms radius of less than $5 \mu\text{m}$. The Strehl ratio is shown in Fig. 12(c). Since the optical system lacks the FoV between 0° and 55° , Fig. 12(c) only makes sense in the part after 55° , i.e., the part surrounded by the dotted line. The Strehl ratio of 486.1 nm light decreases to 0.65 at around 117° FoV, but the average of the three spectra is still above 0.8, and the overall aberration is small. The optical system uses the equidistant projection rule. In order to avoid the interference of the FoV of $(0^\circ - 55^\circ)$, we use Eq. (8) to fit the actual f distortion curve of the optical system. Figure 12(d) shows that the maximum distortion of the annular FoV is only 2%

$$f - \theta \text{ distortion} = \frac{y' - y}{y} \cdot 100\%, \quad (8)$$

where y is the ideal height, i.e., the product of the focal length and FoV, and y' is the actual imaging height.

C. Supplement and Optimization of Transmission Structure

As illustrated in Fig. 11, the central area of the first surface of the PAL has no light, thereby leaving room for light from the forward FoV to enter the PAL. The minimum half-field angle of the annular FoV is 55° , and the half-forward FoV must be approximately 55° to completely eliminate the blind zone. Therefore, the fish-eye lens of the reversed telephoto telecentric structure is required for the front lens group to compress the beam from the forward FoV. In addition, the front lens group also undertakes the function of correcting the focal length and aberration of the forward FoV. To completely eliminate the blind zone, we set the half-forward FoV angle to 56° , which is slightly larger than the minimum half-field angle of the annular FoV. Notably, the focal length of the forward FoV must be smaller than that of the annular FoV to prevent the images of the forward and annular FoVs from overlapping on the focal plane. We constrain the focal length of the forward FoV to

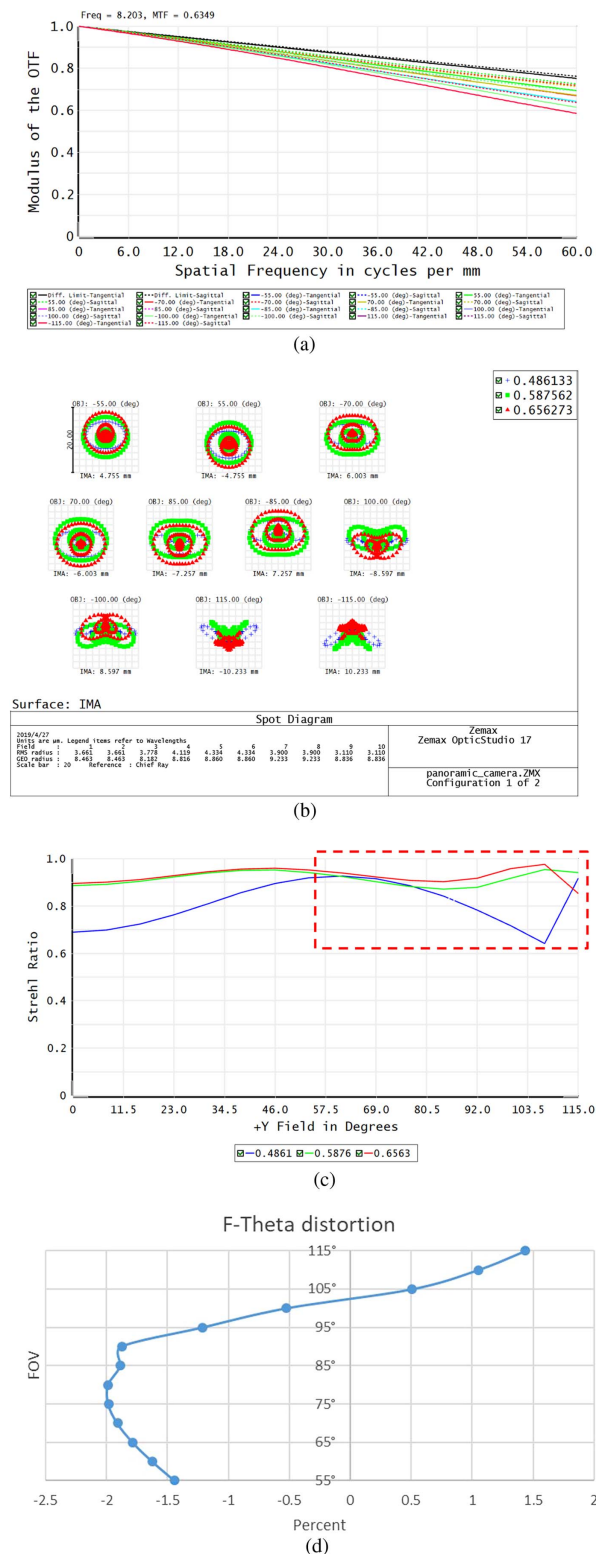


Fig. 12. Image quality of annular FoV: (a) MTF, (b) spot diagram, (c) Strehl ratio, and (d) f -theta distortion.

3 mm. As shown in Eq. (4), the images of the two FoVs have a margin of 1.87 mm on the focal plane and will not interfere with each other. In optimizing the forward structure, the PAL and the relay lens should remain unchanged, and only

the front lens group should be optimized. After supplementing the forward FoV, the overall structure of the extremely wide-angle optical system integrated with transmission and foldback is shown in Fig. 13.

The MTF, spot diagram, Strehl ratio, and distortion curve of the forward FoV are shown in Figs. 14(a)–(d), respectively. The MTFs of forward FoV are higher than 0.62 at 45.5 l/p/mm and 0.48 at 60 l/p/mm. The rms radius of all spots is also less than 4 μ m, and the Strehl ratio of all fields is about 0.8. Although the Strehl ratio decreased near the largest FoV, the average of the three wavelengths was still above 0.8. The f -theta distortion is less than 1%. Table 1 provides the major parameters of the lens.

The two FoVs of the optical system use the same sensor, and so it must ensure that the images of the two FoVs will not overlap. The theoretical distance of the two images is 1.87 mm on the focal plane, but the actual distance may be different from the design value because of the existence of aberration. The spot diagrams [Fig. 12(b) and Fig. 14(b)] show that the imaging height of the minimum field angle of the annular FoV is 4.755 mm and the maximum field angle of the forward FoV is 2.933 mm. So the image of two FoVs has a gap of 1.822 mm on the focal plane, and since the geometric diameter of the spots of both FoVs is less than 20 μ m, the images of two FoVs will not overlap on the focal plane. In addition, in order to avoid the interference of stray light, the coating position of the PAL must be precisely controlled to ensure that the PAL can only transmit the beam of the required FoV rather than the other FoV. And, other lenses need to be coated with antireflection film to prevent stray light reflection between the lenses.

D. Sensitivity Analysis of Focal Plane Position

When using an optical system, we need to adjust the position of the focal plane to get the clearest image. The optical system designed in this paper has two FoVs with different focal lengths, and the positions of the best focal planes for the two FoVs may be slightly different. The system is a telecentric structure, which reduces the sensitivity of the focal plane

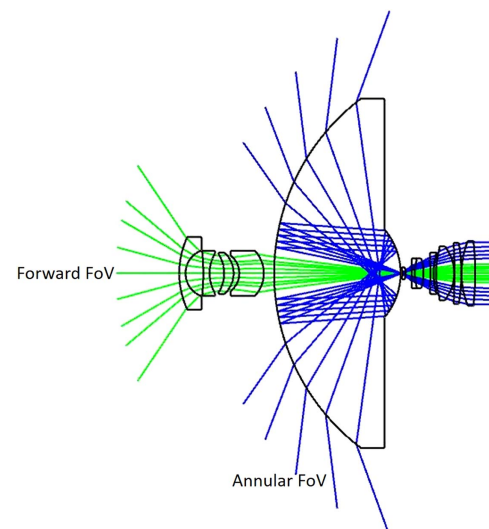
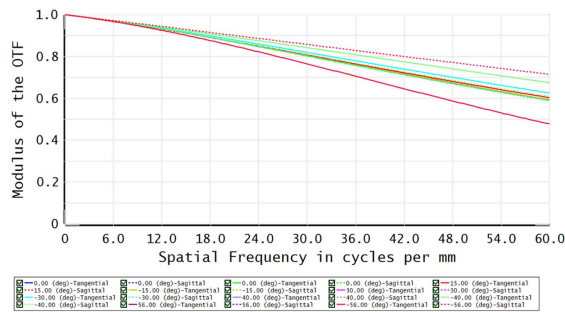
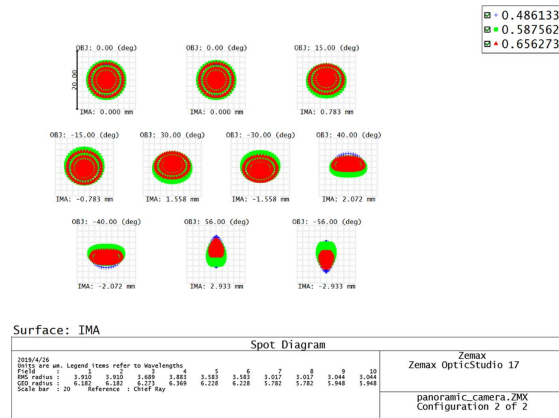


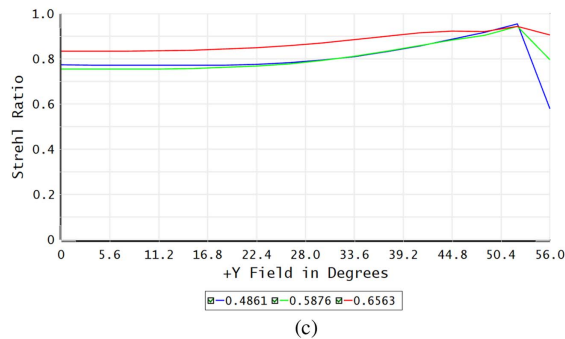
Fig. 13. Overall optical system integrated with transmission and foldback.



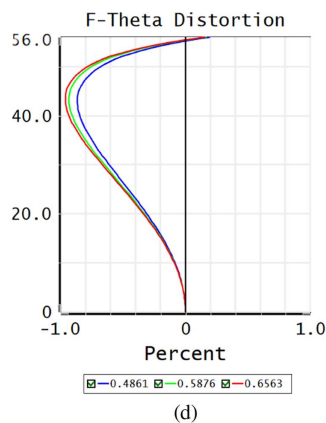
(a)



(b)



(c)



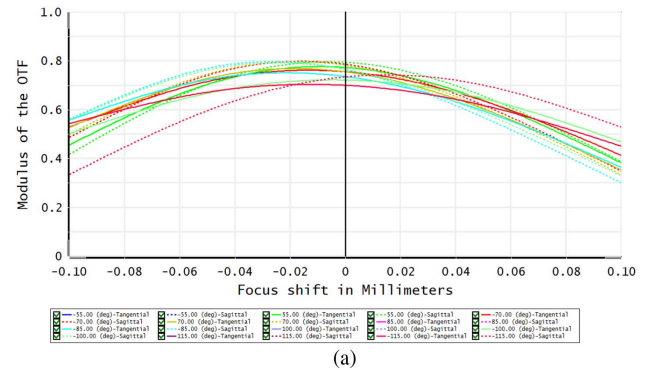
(d)

Fig. 14. Image quality of forward FoV: (a) MTF, (b) spot diagram, (c) Strehl ratio, and (d) f -theta distortion.

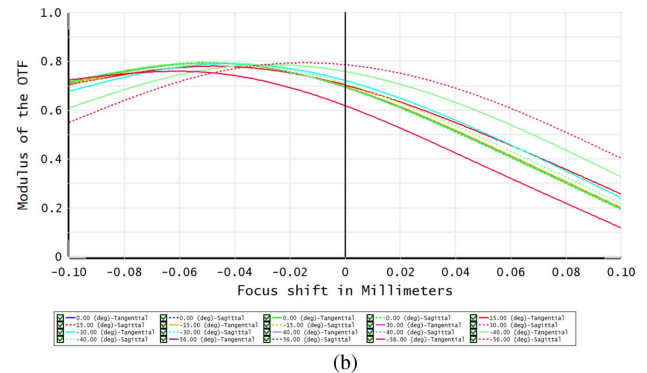
position to a certain extent. Figure 15(a) shows the through-focus MTF of annular FoV. At the Nyquist frequency, the focal plane of the annular FoV moves 0.1 mm before and after, and

Table 1. Major Parameters of the Extremely Wide-Angle Lens Integrated with Transmission and Foldback

Parameters	Forward FoV	Annular FoV
Total FoV	230°	
Bands	F, d, C (486.1 nm, 587.6 nm, 656.3 nm)	
Partial FoV	$360^\circ \times (0^\circ\text{--}56^\circ)$	$360^\circ \times (55^\circ\text{--}115^\circ)$
Focal length	3 mm	5 mm
F number	5	5
F -theta distortion	<1%	<2%
MTF @60 l p/mm	>0.48	>0.58



(a)



(b)

Fig. 15. Through-focus MTF of imaging system: (a) annular FoV and (b) forward FoV.

the MTF remains above 0.3. Figure 15(b) shows through-focus MTF of the forward FoV. The MTF increases when the focal plane moves forward, which indicates that the forward FoV has a slight defocus. When the focal plane is shifted by 0.1 mm in front or 0.06 mm in back, the MTF remains above 0.5 and 0.3, respectively. The currently mounting accuracy of the lens can be accurate to 0.01 mm, and the imaging quality of the optical system is less sensitive to the focal plane position, and so a focal plane position for good imaging of both FoVs can be found.

5. MECHANICAL STRUCTURE

The extremely wide-angle lens with integrated transmission and foldback has two FoVs. In addition, the beams of two FoVs enter the optical system from various entrance pupils. If the conventional lens cone is used, then the lens cone will block the beam from the annular FoV. The lens cone of the

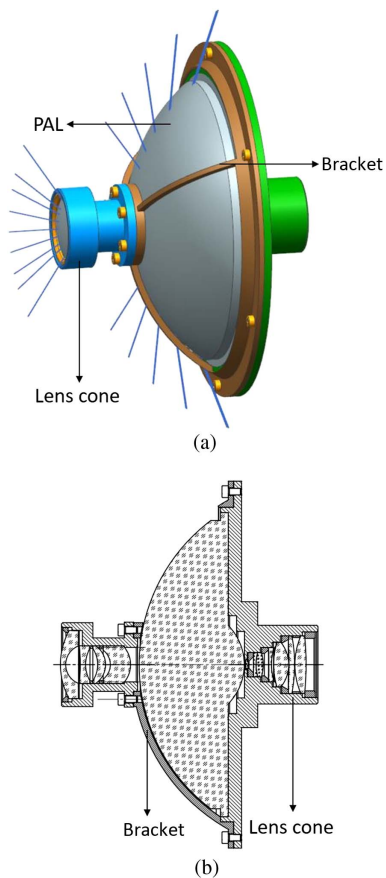


Fig. 16. Mechanical structure of the extremely wide-angle lens: (a) 3D stereogram and (b) cutaway view.

frame structure is designed in this study. As shown in Fig. 16, the lens cone is divided into three parts, which are equipped with the front lens, the PAL, and the relay lens. Screws are used to connect the three parts of the lens cone. This lens cone is similar to the lens cone of the Cassegrain telescope, which fixes the secondary mirror using three brackets and allows light to enter the system from the gaps between the brackets. The lens cone of the extremely wide-angle lens is also connected to the front lens group and the PAL via three brackets. The light of the forward FoV enters from the front lens, whereas that of the annular FoV enters the PAL from the brackets gap. The inner wall of the lens cone is coated with absorptive medium to absorb stray light by means of the roughness and porous scattering of the medium.

6. CONCLUSION

An extremely wide-angle lens integrated with transmission and foldback is designed in this study based on the imaging principles of fish-eye and catadioptric wide-angle lenses. The total FoV of the designed lens is 230° , with a forward FoV of $360^\circ \times (0^\circ\text{--}56^\circ)$ and an annular FoV of $360^\circ \times (55^\circ\text{--}115^\circ)$. The lens achieves good imaging quality when all the optical elements used are only ordinary spherical lenses, thereby proving the imaging advantage of this system in a large FoV. If the FoV

requires further expansion, then the lens can be further optimized from the following aspects.

1. The number of surfaces of the PAL should be increased. For example, the number of surfaces with different curvatures should be increased to four.
2. The spherical surfaces of the PAL should be replaced with aspherical or free-form surfaces.
3. Allocating the spatial extent of the two FoVs is more reasonable. For example, the maximum field angle of the forward FoV and the minimum field angle of the annular FoV can be simultaneously increased.

The newly designed optical structure preserves the advantages of large FoVs of a catadioptric wide-angle lens and completely eliminates the blind areas of small FoVs. The optical system has extensive application prospects in many fields, such as space detection, virtual environment navigation, and 3D surveillance.

Funding. Youth Innovation Promotion Association of the Chinese Academy of Sciences; National Science Foundation for Young Scholars of China (61505203); National Key Research and Development Plan of China (2016YFB0502605); Key Scientific and Technological Research and Development Projects of Jilin (20180201109GX); Scientific and Technological Plan of Changchun (18SS012).

REFERENCES

1. V. A. Solomatin, "A panoramic video camera," *J. Opt. Technol.* **74**, 815–817 (2007).
2. Z. Zhu, E. M. Riseman, and A. R. Hanson, *Geometrical Modeling and Real-Time Vision Applications of a Panoramic Annular Lens (PAL) Camera System* (University of Massachusetts, 1999).
3. L. Zhao, H. Feng, J. Bai, X. Liu, and H. Li, "An improved image restoration method for the high definition panoramic camera system," *Opt. Laser. Eng.* **47**, 982–989 (2009).
4. W. Li and Y. F. Li, "Single-camera panoramic stereo imaging system with a fisheye lens and a convex mirror," *Opt. Express* **19**, 5855–5867 (2011).
5. J. Kannala and S. S. Brandt, "A generic camera model and calibration method for conventional, wide-angle, and fish-eye lenses," *IEEE Trans. Pattern Anal. Mach. Intell.* **28**, 1335–1340 (2006).
6. G. Jang, S. Kim, and I. Kweon, "Single-camera panoramic stereo system with single-viewpoint optics," *Opt. Lett.* **31**, 41–43 (2006).
7. D. Schneider, E. Schwalbe, and H. G. Maas, "Validation of geometric models for fisheye lenses," *ISPRS. J. Photogr.* **64**, 259–266 (2009).
8. C. B. Martin, "Design issues of a hyperfield fisheye lens," *Proc. SPIE* **5524**, 84–92 (2004).
9. D. Hui, M. Zhang, Z. Geng, Y. Zhang, J. Duan, A. Shi, L. Hui, Q. Fang, and Y. Liu, "Designs for high performance PAL-based imaging systems," *Appl. Opt.* **51**, 5310–5317 (2012).
10. S. Thibault, "Panoramic lens applications revisited," *Proc. SPIE* **7000**, 70000L (2008).
11. Y. Luo, J. Bai, X. Zhou, X. Huang, Q. Liu, and Y. Yao, "Non-blind area PAL system design based on dichroic filter," *Opt. Express* **24**, 4913–4923 (2016).
12. J. Wang, Y. Liang, and M. Xu, "Design of panoramic lens based on ogive and aspheric surface," *Opt. Express* **23**, 19489–19499 (2015).
13. E. C. Driscoll, Jr., E. P. Wallerstein, W. C. Lomax, J. E. Parris, J. L. W. Furlan, E. V. Bacho, and J. E. Carbo, Jr., "Panoramic imaging arrangement," U.S. patent 6,341,044 (22 January, 2002).
14. M.-J. Sheu, C.-W. Chiang, W.-S. Sun, J.-J. Wang, and J.-W. Pan, "Dual view capsule endoscopic lens design," *Opt. Express* **23**, 8565–8575 (2015).

15. M. Mizusawa, "Wide angle optical system," U.S. patent 9,810,886 (7 November, 2017).
16. I. Powell, "Panoramic lens," U.S. patent 5,473,474 (5 December 1995).
17. X. Zhou, J. Bai, C. Wang, X. Hou, and K. Wang, "Comparison of two panoramic front unit arrangements in design of a super wide angle panoramic annular lens," *Appl. Opt.* **55**, 3219–3225 (2016).
18. A. M. Samy and Z. Gao, "Simplified compact fisheye lens challenges and design," *J. Opt.* **44**, 409–416 (2015).
19. H. Zhi, J. Bai, and X. Y. Hou, "Design of panoramic stereo imaging with single optical system," *Opt. Express* **20**, 6085–6096 (2012).10.1364/OE.20.006085
20. Y.-H. Huang, Z.-Y. Liu, Y.-G. Fu, and H. Zhang, "Design of a compact two-channel panoramic optical system," *Opt. Express* **25**, 27691–27750 (2017).